J Solid State Electrochem (1999) 3: 277–287

ORIGINAL PAPER

Alar Jänes · Peep Miidla · Enn Lust

Adsorption of 1-pentanol on bismuth single-crystal plane electrodes

Received: 1 July 1998 / Accepted: 2 October 1998

Abstract Cyclic voltammetry, impedance and chronocoulometry have been employed for the quantitative study of 1-pentanol (*n*-PenOH) adsorption at the bismuth single-crystal plane | aqueous Na_2SO_4 solution interface. The adsorption isotherms, Gibbs energies of adsorption ΔG°_{A}, the limiting surface excess Γ_{max} and other adsorption parameters, dependent on the crystallographic structure of the electrodes, have been determined. The adsorption of *n*-PenOH on Bi single-crystal planes is mainly physical and is limited by the rate of diffusion of organic molecules to the electrode surface. Comparison of the adsorption data for *n*-PenOH with 1-propanol (*n*-PrOH), 1-butanol (*n*-BuOH), cyclohexanol (CH) and 1-hexanol (*n*-HexOH) shows that the adsorption characteristics depend on the structure of the hydrocarbon group. The adsorption activity of adsorbates at the bismuth | solution interface increases in the sequence *n*-PrOH < *n*-BuOH < CH ≤ *n*-PenOH < *n*-HA as the adsorption activity at the air | solution interface increases. For all the compounds studied, the adsorption activity increases in the sequence of planes (111) < (001) < (01$\bar{1}$).

Key words Cyclic voltammetry · Impedance · Chronocoulometry · 1-Pentanol

Introduction

This work is a part of the project devoted to the study of the influence of the crystallographic structure of bismuth on the adsorption of neutral organic molecules at the Bi | solution interface [1–9]. Adsorption of various organic compounds at the polycrystalline bismuth solid drop electrode (BDE) has been described previously [10–15]. The statistical treatment of the electron diffraction studies and capacity data shows that the surface of the BDE consists mainly (ca. 60%) of homogeneous segments whose crystallographic, double layer and adsorption characteristics are similar to those for the (001) plane of bismuth [10, 16].

The electrosorption behaviour of the same aliphatic compounds from electrolyte solutions on different metals under otherwise identical conditions may provide further useful information on the role played by metal-water and water-water interactions upon electrosorption [1–25]. In fact, the chemical nature and crystallographic structure of the single-crystal plane electrode is known to affect the structuring of interfacial water molecules, which has been studied extensively from both experimental and theoretical points of view [1–9, 17–29]. Systematic adsorption measurements of *n*-aliphatic alcohols and their isomers from aqueous electrolyte solutions have been carried out on various *sp* metals, such as Hg, Pb, Bi, Cd, Sn, Sb, Zn, In-Ga and Ga [10–15, 19–25, 30–40]. In general, these measurements indicate that the adsorption of aliphatic compounds is weaker the more hydrophilic is the metal. Comparison of the adsorption data of 1-propanol (*n*-PrOH), 1-butanol (*n*-BuOH), cyclohexanol (CH) and 1-hexanol (*n*-HexOH) shows that the difference of the adsorption parameters for various planes increases as the adsorption activity of the adsorbate at the air | solution interface, as well as at the electrode | electrolyte solution interface, rises [8, 36, 37, 41–43]. This is mainly caused by the fact that with decreasing the molar volume of adsorbate the transformations in the adsorption layer structure, caused by the adsorption of one surfactant molecule, decrease in comparison with the situation when the adsorption of very large particles takes place. The adsorption studies of various butanol isomers [6] shows that the adsorption parameters depend on the geometrical structure of the

A. Jänes (✉) · E. Lust
Institute of Physical Chemistry,
University of Tartu,
2 Jakobi Street, EE-2400 Tartu, Estonia
e-mail: alar@ut.ee

P. Miidla
Institute of Applied Mathematics,
University of Tartu,
2 Liivi Street, EE-2400 Tartu, Estonia

hydrocarbon tail of the adsorbate, and thus comparison of the adsorption behaviour of 1-pentanol (*n*-PenOH) with CH would provide more information on the influence of the hydrocarbon chain structure on the adsorption process and about the attractive interactions in the adsorbed layer. However, a further difficulty in the comparison of results from different laboratories lies in the fact that different experimental techniques are often used [19–22].

For a more profound understanding of the importance of the crystallographic structure of the electrode surface and the geometrical structure of the hydrocarbon chains of adsorbate in the adsorption phenomena, in the present work we investigated the adsorption of *n*-PenOH on singular (111), (001) and (00$\bar{1}$) faces of bismuth and compared the parameters obtained with the adsorption data of various organic compounds on Bi planes [1–9].

Experimental

The experimental procedure used in this work has been described previously [1–9]. The electrode surface was electrochemically polished in aqueous KI + HCl solution at a current density $i \leq 1.5$ A cm^{-2}. Thereafter, a second X-ray diagram was used to determine the precise angle, and only those samples whose precision on the orientation was better than $\pm 0.10^{\circ}$ were used for electrochemical investigations. After the electrochemical polishing, the electrodes were very well rinsed with ultra purified water and were polarised at -1.0 V versus a saturated calomel electrode (SCE) in the working surface-inactive solution.

For additional characterisation of the working surface of the electrodes, electron microscopic analysis by JEOL-JSM-35CF at the SEI regime was made (40000× max.). According to these measurements, the electrochemically polished surfaces of the bismuth electrodes were smooth (naturally within the range of the sensitivity of electron microscopy) [5].

Water for preparing the solutions was treated with the Milli Q+ purification system. Solutions were prepared volumetrically using Na_2SO_4 purified by triple recrystallization from water, and treated in vacuum to dryness. Na_2SO_4 was calcined at 700 °C immediately prior to the measurements. Electrolytic hydrogen was bubbled for 1–2 h through the electrolyte before submersion of the electrode into the solution and the temperature was kept at 298 K. 1-Pentanol was purified according to Weissberger [44].

Results and discussion

Cyclic voltammograms

The cyclic voltammograms (CVs) were recorded in order to determine the quality of the surfaces investigated and the potential range in which the adsorption of *n*-PenOH occurred. The shape of the CV recorded for the supporting electrolyte was characteristic of the bismuth single-crystal [1–9] and the electrodes investigated were ideally polarizable in the potential range of -1.8 to -0.35 V (SCE) in aqueous 0.05M Na_2SO_4 solution.

Differential capacity versus potential curves (*C*-*E* curves)

The edl (electrical double layer) differential admittance was measured at ac frequencies ν from 60 to 21000 Hz. The capacity dispersion with ν is small in the proximity of the differential capacity minimum (in the region of maximum adsorption), whereas it increases noticeably in the region of the adsorption-desorption peaks. Comparison of the $(C^{\max} - C_0)$ versus $\omega^{1/2}$ curves ($C^{\max}$ = differential capacity at the potential of the adsorption-desorption maximum E^{m}; C_0 = differential capacity at E^{m} in the base electrolyte; $\omega = 2\pi\nu$) for *n*-PrOH, *n*-BuOH, CH, *n*-PenOH and *n*-HexOH shows that this dependence increases with the rise of the molecular weight and the molar volume of the adsorbate. As shown in elsewhere [24, 45], if the rate of adsorption of organic compounds is limited by diffusion, the equilibrium values of differential capacity at $\nu = 0$ can usually be found with a sufficient degree of accuracy by extrapolation of the C_{add}-$\omega^{1/2}$ curve to $\omega^{1/2} = 0$. According to the experimental results, in the region of $60 < \nu < 710$ Hz, the C_{add}-$\omega^{1/2}$ curves have a good linearity and, accordingly, we can obtain the equilibrium values of differential capacity.

According to the method described elsewhere [24, 45–47], the equilibrium values of differential capacity can be calculated by Eq. (1):

$$C_{\mathrm{add}}(\omega = 0) = C^2_{\mathrm{add}}(\omega) R^2_{\mathrm{p}}(\omega) \omega^2 + 1/\left\{ \left[C_{\mathrm{add}}(\omega) R_{\mathrm{p}}(\omega) \omega - 1 \right] R_{\mathrm{p}}(\omega) \omega \right\} \quad (1)$$

where $C_{\mathrm{add}}(\omega)$ and $R_{\mathrm{p}}(\omega)$ are the values of differential (additional) capacity and parallel resistance at $\omega = \mathrm{const}$. The components of the adsorption impedance were calculated from the impedance data of the cell used for the measurements (series circuit), i.e. $C_{\mathrm{S}}(\omega)$ and $R_{\mathrm{S}}(\omega)$, following described procedure [24, 45–47]. By extrapolating the $R_{\mathrm{S}}(\omega)$ values to $\omega \to \infty$ the solution resistance $R_{\mathrm{S}}(\omega) = R_{\mathrm{sol}}$ was determined. Since the amount of organic compounds added is small and does not affect the solution resistance, one can assume R_{sol} to be equal to the ohmic component R_{S} of the impedance in the pure base electrolyte solution. The values of R_{sol} and R_{S} obtained in this work are in good agreement with previous data [6, 48]. Then the series equivalents $R_{\mathrm{S}}(\omega) - R_{\mathrm{sol}}$ and $C_{\mathrm{S}}(\omega)$ of the impedance were converted into the parallel equivalents $C_{\mathrm{P}} + C_{\mathrm{true}}$ and R_{P} using known relations [24, 45–47].

The equilibrium values of $C_{\mathrm{add}}(\omega = 0)$ for the 0.04 M *n*-PenOH + 0.05 M Na_2SO_4 system, calculated by Eq. 1, at E^{m} are 60–64, 54–62 and 53–60 μF cm^{-2} for Bi(001), Bi(111) and Bi(01$\bar{1}$), respectively. These values are in good agreement with the values obtained from C_{add}-$\omega^{1/2}$ curves at the condition $\omega^{1/2} = 0$ [58 ± 5.0 μF cm^{-2} for Bi(111), 63 ± 5.0 μF cm^{-2} for Bi(001) and 56 ± 5.0 μF cm^{-2} for Bi(01$\bar{1}$)].

All the C-E curves ($\omega = 0$) determined in the presence of n-PenOH in the solutions investigated merge with the curve for the supporting electrolyte at -1.8 V (SCE) (Fig. 1), indicating that n-PenOH molecules are completely desorbed from the bismuth surface at these negative potentials. At less negative potentials the C-E curves display the characteristic adsorption-desorption peaks. The height of the peak increases and its potential shifts to the negative direction with increasing n-PenOH concentration. As we can see from Fig. 1 and Fig. 2, the shape (the height and width) of the adsorption-desorption maximum at $c_{org} = \text{const.}$ depends on the geometrical structure of the adsorbate hydrocarbon chains. At $E < E_{\sigma=0}$ the attractive interaction constant a^m obtained according to the Frumkin-Damaskin theory [24, 27] increases in the sequence n-PrOH < n-BuOH < n-PenOH < n-HexOH < CH. Thus the attractive interaction between the adsorbed molecules increases in the same order of the compounds. The potential of the adsorption-desorption maximum E^m at $E < E_{\sigma=0}(c_{org} = \text{const.})$ depends on the geometrical structure of the adsorbate, and the adsorption activity of adsorbates increases in the sequence of n-PrOH to n-HexOH (Fig. 3). The height and potential of the adsorption-desorption peaks depend on the geometrical structure of the electrode surface (Fig. 4). According to the experimental data, these maxima increase in height in the sequence of faces $(01\bar{1}) < (111) \leq (001)$. Accordingly, the attractive interaction constant a^m at E^m increases as the superficial density of the atoms decreases. The same tendency is valid for n-PrOH, n-BuOH, CH and n-HexOH adsorption at the Bi single-crystal plane electrodes [1–9].

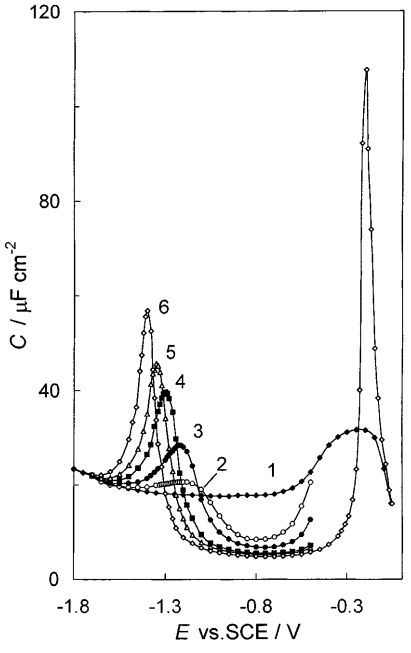

Fig. 1 C-E curves ($\omega = 0$) for Bi(111) in 0.05 M Na_2SO_4 (*1*) and with addition of 1-pentanol (M): 0.02 (*2*); 0.03 (*3*); 0.05 (*4*); 0.07 (*5*); 0.1 (*6*)

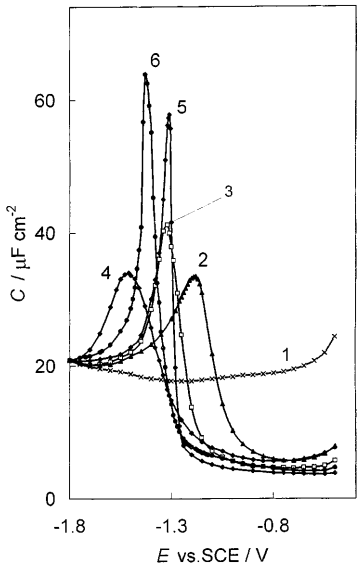

Fig. 2 C-E curves ($\nu = 210$ Hz) for Bi(001) in 0.05 M Na_2SO_4 (*1*) and with addition of various alcohols: n-BuOH (*2, 4*); n-PenOH (*3*); CH (*5*); n-HexOH (*6*)

At $E \approx E_{\sigma=0}$ the differential capacity decreases to a value much smaller than that observed for the pure base electrolyte. The potentials of capacity minimum of the C-E curves E_{max} are independent of the concentration of adsorbate, indicating that the orientation of adsorbed n-PenOH molecules is practically independent of the surface coverage θ in the region of maximum adsorption. The values of the limiting capacity C_1 at the surface coverage $\theta = 1$ at $E = E_{max}$, obtained by the extrapolation of the linear dependence of $1/C$ on $1/c_{org}$ to $1/c_{org} = 0$ (c_{org} = concentration of organic compound in solution), increase in the order of planes $(001) < (111) < (01\bar{1})$ (Table 1). According to the Helmoltz equation for the plate condenser, $C = \varepsilon\varepsilon_0/d$ (where ε and ε_0 are the dielectric constants of the medium and vacuum, respectively, and d is the thickness of the adsorbed layer), the decrease of C_1 can be explained by the decrease of ε caused by the increase of the amount

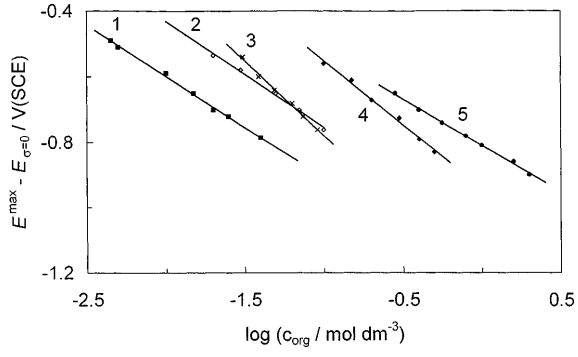

Fig. 3 Dependence of the difference between the potential of the adsorption-desorption maximum and the zero charge potential ($E^{max} - E_{\sigma=o}$) on log c_{org} at Bi(111) for various organic compounds: n-HexOH (*1*); n-PenOH (*2*); CH (*3*); n-BuOH (*4*); n-PrOH (*5*)

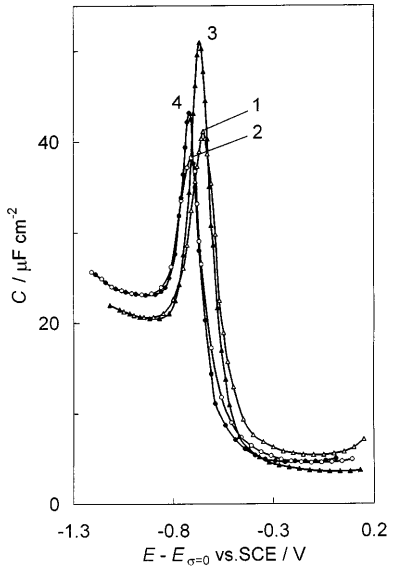

Fig. 4 *C-E* curves ($\nu = 210$ Hz) for Bi(111) (*1, 3*) and for Bi(011) (*2, 4*) with addition of 0.05 M *n*-PenOH (*1, 2*) and 0.01 M *n*-HexOH (*3, 4*)

of organic compound in the adsorbed layer, as well as by the increase of the adsorbed layer thickness, which may be caused by the more vertical orientation of the adsorbed molecules. The same order of the dependence of C_1 on the crystallographic structure of the electrode surface is valid for *n*-PrOH, *n*-BuOH, CH and *n*-HexOH adsorption at Bi electrodes.

The adsorption-desorption maxima at $E^m > E_{\sigma=0}$ for *n*-PenOH were found at $-0.4 < E < -0.10$ V (SCE). For more concentrated solutions of *n*-PenOH ($c_{org} > 0.08$ M), the peaks lie at very positive potentials [$E > -0.25$ V (SCE)] and are probably distorted by a slight specific adsorption of the anions [2–8]; therefore, they were not used for the calculation of the adsorption parameters. As in the region of potentials $E^m < E_{\sigma=0}$, the heights of the peaks at $E^m > E_{\sigma=0}$ increase in the order of planes $(01\bar{1}) < (111) \leq (001)$, but the maxima at $E^m > E_{\sigma=0}$ are noticeably narrower than those at $E < E_{\sigma=0}$. Thus, the attractive interaction at $E > E_{\sigma=0}$ is somewhat higher than that for a negatively charged surface.

Charge density-potential curves

The charge density-potential σ_0-E curve for a base electrolyte solution was obtained by the integration of the *C-E* curve ($\omega = 0$), starting from the potential of zero charge $E_{\sigma=0}$ [1–9]. The charge density-potential curves for solutions with different additions of adsorbate were obtained by back integration of the *C-E* curves ($\omega = 0$), starting from $E = -1.8$ V (SCE) and assigning the value of σ ($E = -1.8$ V) equal to σ_0 ($E = -1.8$ V), because there is no adsorption at $E = -1.8$ V (SCE). The shape of σ-E curves is typically observed for the adsorption of neutral organic molecules at ideally polarisable electrodes [2–9] (Fig. 5) and will be discussed later.

The values of the initial and final potentials for the potential step chronocoulometric experiments were chosen with the help of the *C-E* and cyclic voltammetric *i-E* curves. The initial potential E_i was varied from -0.40 to -1.80 V (SCE). The final potential E_f was equal to -1.60 V (SCE) for $c_{org} \leq 0.005$ M and -1.80 V (SCE) for $c_{org} > 0.005$ M. This value was chosen carefully in order to: (1) achieve the complete desorption of *n*-PenOH and (2) keep the current of hydrogen evolution small enough so that the faradaic reaction would not interfere with the determination of the electrode charge density (σ) [6, 7, 19–22, 30, 49, 50]. Five series of step experiments were made for *n*-PenOH concentrations from 5×10^{-3} to 1×10^{-1} M. The σ-E curves were calculated according to method described by Lipkowski et al. [51–54]. The precision of charge measurements is about 2–3%.

The σ-E curves for the different concentrations of *n*-PenOH investigated intersect the curve obtained for the base electrolyte (Fig. 5). The comparison of the σ-E

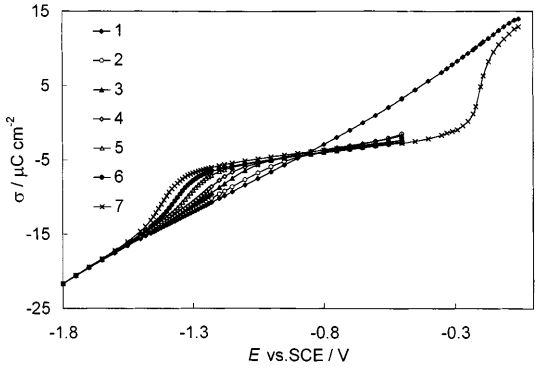

Fig. 5 σ-E curves obtained from impedance ($\omega = 0$) for Bi(001) in 0.05 M Na_2SO_4 (*1*) and with addition of *n*-PenOH (M): 0.01 (*2*); 0.02 (*3*); 0.03 (*4*); 0.05 (*5*); 0.07 (*6*); 0.10 (*7*)

Table 1 Adsorption parameters of 1-pentanol on Bi single-crystal planes (chronocoulometry data, except C_1, a_m and B_m obtained by impedance method at $\omega = 0$)

Plane	a_m ± 0.1	C_1 ± 0.15 (μF cm^{-2})	S_{max} ± 0.02 (nm^{-2})	$10^{10}\,\Gamma_{max}$ ± 0.4 (mol cm^{-2})	E_N ± 0.04 (V/SCE)	B ± 5 (dm^3 cm^{-2})	$-\Delta G^\circ_{ads}$ ± 0.3 (kJ mol^{-1})
(111)	1.42	3.9	0.33	5.4	0.40	17.1	17.0
(001)	1.37	3.6	0.37	5.1	0.36	20.0	17.4
(01$\bar{1}$)	1.32	3.7	0.49	4.9	0.24	41.3	19.2

data for the capacitance and potential step measurements shows that the difference between the values of σ, obtained by these different methods, does not exceed ± 0.75 μC cm^{-2}, which is only slightly higher than the experimental error for obtaining the σ values. The small deviation of the σ-E curves, obtained from impedance, from the chronocoulometric σ-E curves indicate that in spite of the extrapolation of C-E curves to $\omega = 0$, these curves are non-equilibrial. Comparison of the charge-potential data for *n*-PrOH, *n*-BuOH, CH, *n*-HexOH and *n*-PenOH [5, 6, 8, 9, 48] shows that the difference between σ values obtained by these methods increases in the sequence of adsorbates *n*-PrOH < *n*-BuOH < *n*-PenOH < CH < *n*-HexOH as the adsorption activity of the organic compound at the electrode increases. Therefore, the quantitative data, presented in this work, are mainly obtained from the chronocoulometric measurements. The potential at which the curves intersect is the potential of maximum adsorption E_{max}. As we can see from Fig. 5, E_{max} is practically independent of c_{ads} and the values of E_{max} are equal to -0.90, -0.85 and -0.80 V for Bi(111), Bi(001) and Bi(01$\bar{1}$) planes, respectively. These values of E_{max} are in good agreement with the potentials of capacity minimum of the C-E curves. The charge density σ_{max}, at which the maximum adsorption takes place, slightly depends on the plane, and the absolute value of σ_{max} decreases in order (01$\bar{1}$) < (001) < (111) (σ_{max} is equal to 4.5, 5.0 and 6.0 μC cm^{-2}, respectively). The nearly linear segments were observed on the σ-E curves close to E_{max}. By linear extrapolation of these fragments of the curve to $\sigma = 0$, the potentials of zero charge corresponding to the surface covered by adsorbate molecules have been obtained. The difference between these values and the value of $E_{\sigma=0}$ for the pure base electrolyte solution is equal to the change in the surface potential due to the displacement of a monolayer of water molecules by a monolayer of *n*-PenOH (E_N). The established values of E_N are presented in Table 1. These quantities are related by the following equation derived from the model of two parallel capacitors [24]:

$$E_{max} - E_{\sigma=0} = -E_N C_1/(C_0 - C_1);$$
$$\sigma_{max} = -E_N C_1 C_0/(C_0 - C_1) \quad (2)$$

The calculations show that the values of E_N increase in the sequence of Bi planes (01$\bar{1}$) < (001) < (111), and this is in good agreement with the decrease of absolute values of σ_{max} in the sequence of the planes (111) > (001) > (01$\bar{1}$). The same order of planes is valid for *n*-PrOH, *n*-BuOH, CH and *n*-HexOH adsorption at Bi planes [1–6, 8, 9, 48]. With the help of the unrationalized Helmholtz formula, E_N can be expressed as

$$E_N = \Gamma_{max}(\mu^{org} - n\mu^w)/\varepsilon\varepsilon_0 \quad (3)$$

where Γ_{max} is the limiting surface excess of *n*-PenOH, μ^{org} and μ^w are the components of the dipole moment normal to the surface of the electrode for the organic compound and H_2O molecules, respectively, $\mu^{org} - n\mu^w = \bar{\mu}_{eff}$ where $\bar{\mu}_{eff}$ is the effective dipole moment, n is the number of H_2O molecules displaced by one adsorbed *n*-PenOH molecule, and ε is the permittivity of the inner layer. The positive sign of E_N indicates that either (1) $|\mu^{org}| > |n\mu^w|$ and $\mu^{org} > 0 (\mu^w <_> 0)$ or (2) $|\mu^{org}| < |n\mu^w|$ and $\mu^{org} < 0$. In the first case, μ^{org} is positive, which means that the molecules of *n*-PenOH are oriented with the hydrocarbon chain facing the Bi surface at E_{max}. In the second case, *n*-PenOH molecules may be oriented with the hydrocarbon tail towards the electrode surface ($\mu^{org} > 0$), as well as the —OH group facing the electrode surface ($\mu^{org} < 0$). In these two latter cases the positive values of E_N would suggest a strong preferential orientation of H_2O with oxygen atoms towards the electrode surface at E_{max} (not far from $E_{\sigma=0}$) with $\mu^w < 0$, which is in contradiction with the data of very weak H_2O adsorption at Bi planes [1–9, 29, 43]. As the maximum adsorption of *n*-PenOH takes place at the negatively charged surfaces, it seems that the first possibility for Bi(111), Bi(001) and Bi(01$\bar{1}$) planes is more plausible. Thus, the effective dipole moment of the organic molecules must be positive and, in the region of potentials of maximum adsorption, *n*-PenOH molecules on bismuth single-crystal planes are oriented with the hydrocarbon radical facing the bismuth surface and the functional —OH group facing the solution side of the interface. The same conclusions are valid if the adsorption of the aliphatic alcohols *n*-PrOH ($E_N = 0.33$ V), *n*-BuOH ($E_N = 0.24$ V), *n*-PenOH ($E_N = 0.21$ V) and *n*-HexOH ($E_N = 0.20$ V) takes place at the Hg electrode from 0.1M NaF aqueous solution [22–24, 30]. The higher values of E_N for the Bi planes indicate that the adsorbed *n*-PenOH molecules have a more vertical orientation on Bi in comparison with that for Hg. The noticeably lower value of E_N for the Bi(01$\bar{1}$) plane probably indicates that a more pronounced horizontal orientation of *n*-PenOH at this chemically most active plane is plausible. The value of E_N depends on the geometrical structure of the hydrocarbon chain of the adsorbate, and the effective dipole moment $\bar{\mu}_{eff}$ increases in the sequence of adsorbates *n*-HexOH < *n*-PenOH < *n*-BuOH < CH < *n*-PrOH [1–8]. Thus, at the Bi planes investigated the *n*-PenOH molecules would have the more horizontal orientation compared with *n*-PrOH or *n*-BuOH molecules adsorbed [3, 5, 6, 8]. The same conclusion is valid for the Hg electrode [23, 24, 30].

Specific surface work and film pressure curves

The C-E curves were twice back-integrated, and the chronocoulometric σ-E curves were once back-integrated to obtain a specific surface work decrease ($\gamma - \gamma_0$) as a function of the electrode potential and adsorbate concentration [5, 7, 8, 19–22, 48]. The second integration was performed from the same negative charge at first, assigning the value of zero to the specific surface work at $E_{\sigma=0}$ in the base solution. A good accordance between ($\gamma - \gamma_0$)-E curves, obtained from capacity-potential

and potential step measurements [$\Delta(\gamma - \gamma_0) = \pm 0.50$ μJ cm^{-2}], can be seen between −22 and 4 μJ cm^{-2}, where the thermodynamic analysis takes place.

The pressure of the film of adsorbate π can be determined as

$$\pi(E) = \gamma_{c=0} - \gamma_c = \int_{E_0}^{E} \sigma_c \, dE - \int_{E_0}^{E} \sigma_{c=0} \, dE \qquad (4)$$

where subscripts c and $c = 0$ indicate the presence or absence of the adsorbate in the bulk of the electrolyte, respectively. The calculated π-E curves are plotted in Fig. 6. For more concentrated solutions of *n*-PenOH ($c \geq 0.003$ M) the curve displays a maximum, the potential of which is practically independent of c_{org}, and this value is in good agreement with the value of E_{max} for C-E curves. The comparison of the π-E curves, obtained from capacity-potential ($\omega = 0$) and potential step measurements, shows that the departure of the Bi | *n*-PenOH system from equilibrium is small under the peak at negative rational potentials. The film pressure of the adsorbate at c_{org} = const. increases in the sequence of compounds *n*-PrOH < *n*-BuOH < *n*-PenOH < *n*-HexOH (Fig. 7). Accordingly, the adsorption activity of the compounds increases in the presented sequence of adsorbates.

The adsorption activity of bismuth electrodes increases in the sequence of planes (111) < (001) < (01$\bar{1}$) as the surface density of the atoms increases [except Bi(111)]. This deviation is evidently determined by the competitive adsorption of water and the organic substance, as well as by the crystallographic and electronic structure of the electrodes. Just as in the case of CH, [1, 2, 5–8, 48] and butanol isomers [6] adsorption, the basal plane (111), where the surface atoms are chemically saturated (electron configuration sp^3d^2) [55], has the lowest adsorption activity. The most active one is the singular face Bi(01$\bar{1}$), where unsaturated covalent bonds are distributed uniformly over the whole surface (s^2p^3).

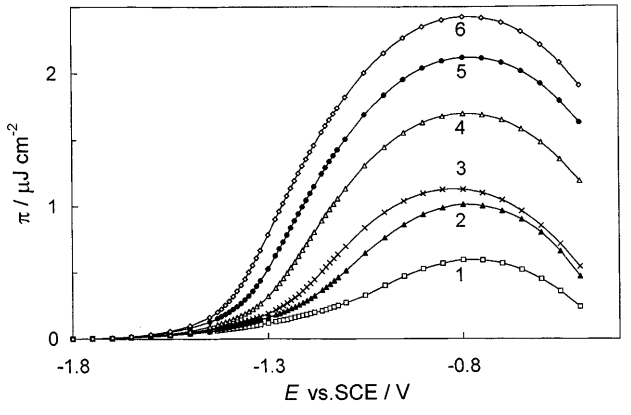

Fig. 6 Surface pressure-potential (π-E) curves for Bi(011) (chronocoulometry) in 0.05 M Na_2SO_4 aqueous solution with addition of *n*-PenOH (M): 0.01 (*1*); 0.02 (*2*); 0.03 (*3*); 0.05 (*4*); 0.07 (*5*); 0.10 (*6*)

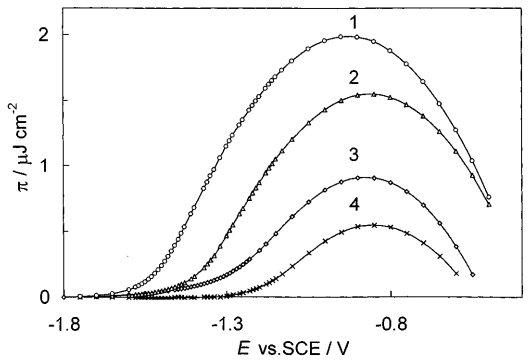

Fig. 7 π-E curves for Bi(001) ($\omega = 0$) in 0.05 M Na_2SO_4 with addition of various alcohols: *n*-BuOH (*1*); *n*-PrOH (*2*); *n*-PenOH (*3*); *n*-HexOH (*4*); (M): 1.5 (*1, 2*); 0.02 (*3, 4*)

Gibbs excess-potential and Gibbs excess-log c_{org} curves

The film pressure data were used to calculate the relative Gibbs surface excess values. First the film pressure was plotted against ln c_{org} at E = const. (Fig. 8). The curves display a long linear section, its slope giving the limiting value of Γ_{max}:

$$\Gamma = \frac{1}{RT}\left(\frac{\partial \pi}{\partial \ln c}\right)_{E,T,P} \qquad (5)$$

As the mole fraction of *n*-PenOH never exceeded 1.5%, at a first approximation, it was assumed that the activity of *n*-PenOH depends linearly on its concentration according to Henry's law [7, 17–28, 56–58]. The values of Γ_{max} obtained for *n*-HexOH are presented in Table 1 and comparison of these data with previous data [2–8, 48] shows that Γ_{max} decreases in the sequence of adsorbates *n*-PrOH > *n*-BuOH > *n*-PenOH > CH > *n*-HexOH as the molar volume of the organic compounds increases. Calculated according to the values of Γ_{max}, the values of the molecular surface area S_{max} (Table 1), corresponding to the area of one adsorbed molecule on the electrode surface at the maximum adsorption potential E_{max}, decrease in the order of Bi planes

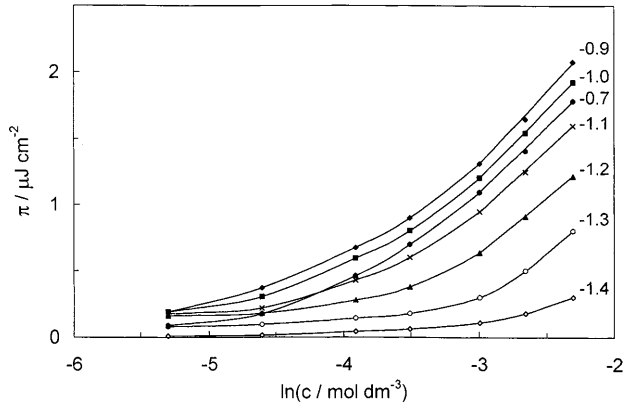

Fig. 8 π-ln c curves for Bi(001) at different electrode potentials, as noted on figure

$(01\bar{1}) > (111) \geq (001)$. If the adsorbed molecules of *n*-PrOH, *n*-BuOH, *n*-PenOH and *n*-HexOH were oriented perpendicularly at the Bi | electrolyte interface, the values of S_{max} should be the same for *n*-PrOH, *n*-BuOH, *n*-PenOH and *n*-HexOH and would be equal to $S_{max}^{theor} \approx 0.21$ nm^2 [24, 25]. The same conclusion would be valid if the orientation of adsorbed molecules is independent of the crystallographic structure of the electrode surface. The increase of the projected area S_{max} as the number of carbon atoms n_C in the hydrocarbon group increases can be explained by the more tilted orientation of the adsorbate molecules on going from *n*-PrOH to *n*-HexOH [7, 8], as well as from Bi(001) to Bi($01\bar{1}$). This conclusion is in good accordance with the noticeable decrease of E_N and $\bar{\mu}_{eff}$ values for *n*-PenOH compared with *n*-PrOH, *n*-BuOH and *n*-HexOH, and with the noticeable decrease of the attractive interaction constant *a* in the sequence of planes Bi(001) $\geq$ Bi(111) > Bi($01\bar{1}$). The same tendency is valid for Ag, Hg and Zn(0001) electrodes if the adsorption of aliphatic alcohols occurs [17–19, 24, 30, 36, 37].

As in the bent region of the π-ln*c* curves the slope changes noticeably and the error of differentiation of the π-ln*c* curves is large [20], the related Gibbs excess values for the intermediate coverages were determined from the electrode charge densities using the well-known formula [21, 24]:

$$\Gamma = \frac{\sigma_\Gamma - \sigma_{\Gamma=0}}{\sigma_{\Gamma_{max}} - \sigma_{\Gamma=0}} \Gamma_{max} \qquad (6)$$

The values of $(\sigma_{\Gamma_{max}} - \sigma_{\Gamma=0})$ were obtained by extrapolation of the linear sections of the σ-*E* curves. The shapes of the Γ-*E* curves for different c_{org} and of the Γ-log*c* curves (Fig. 9 and Fig. 10) suggest that the relative maximum of the adsorption of *n*-PenOH on all the

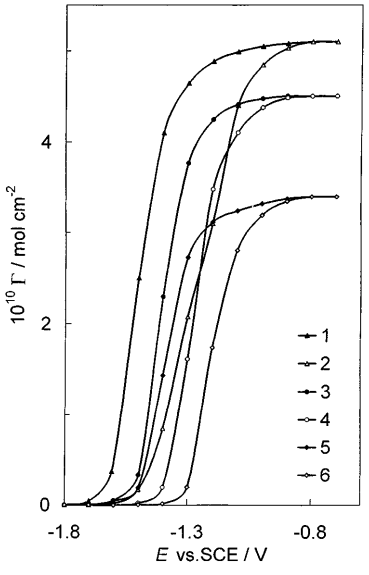

Fig. 9 Gibbs excess-potential (Γ-*E* curves for Bi(111) (*1, 2*); Bi(001) (*3, 4*) and Bi(011) (*5, 6*) with different additions of *n*-PenOH (M): 0.1 (*1, 3, 5*); 0.05 (*2, 4, 6*)

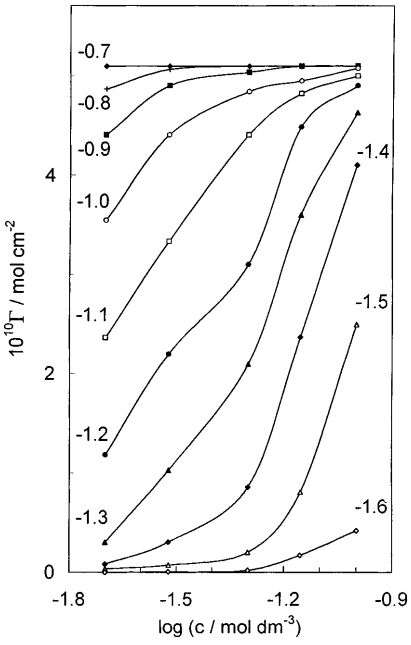

Fig. 10 Γ-log *c* curves for Bi(111) at different electrode potentials [in V (SCE)] as noted on figure

planes investigated is reached at $-0.7 < E < -1.6$ V (SCE) and that Γ_{max} depends on the crystallographic structure of the surface. The values of Γ_{max} increase in the order of electrodes $(01\bar{1}) < (111) < (001)$ and these values are in good accordance with Γ_{max} values obtained from π-ln*c* curves. The slope of the Γ-*E* curves at the region of intermediate values of $\Gamma(c_{org} = \text{const.})$ increases in the order of planes $(01\bar{1}) < (111) < (001)$ and in the order of adsorbates *n*-PrOH < *n*-BuOH < *n*-PenOH < *n*-HexOH < CH as the attraction between the adsorbed molecules rises.

The decrease of Γ_{max} values causes the decrease of the thickness and the effective dielectric constant of the adsorbed layer, and according to the Helmholtz equation it causes the increase of C_1 values in the order of planes Bi(111) < Bi(001) < Bi($01\bar{1}$). The value of Γ_{max} rises in the sequence of electrodes Ag(100) < Ag(111) < Bi($01\bar{1}$) < Bi(111) < Bi(001) < Hg [20, 30].

Adsorption isotherms

The surface coverage at $E = E_{max}$ was first estimated from Eq. 7 based on Frumkin's two parallel condensers model [19, 24, 30]:

$$\theta = (C_0 - C_\theta)/(C_0 - C_1) \qquad (7)$$

Thereafter, at a first approximation, the applicability of the Frumkin isotherm

$$B_m c = \frac{\theta}{1-\theta} \exp(-2a_m\theta) \qquad (8)$$

for the interpretation of *n*-PenOH | Bi data was assumed. In Eq. 8, B_m and a_m are the adsorption equilibrium constant and the molecular interaction

parameter at E_{max}, respectively. The next step is the test of the Frumkin isotherm ($\log[\theta/(1-\theta)c]$ versus θ plot) to derive the adsorption parameters. Figure 11 shows that the plots have a good linearity in the region of $0.1 < \theta < 0.8$ for all the faces investigated. Thus, the slope gives the molecular interaction parameter ($-2a_m$) and the intercept provides the adsorption equilibrium constant $\log B_m$ at E_{max} accordingly.

The adsorption isotherms at various E = const. and at various σ = const. were calculated by the methods described elsewhere [5–10, 17–25, 56–58]. The adsorption isotherms at σ = const. show larger deviations from the Frumkin isotherm behaviour than those at E = const., where the deviations in the region $-0.6 < E < -1.2$ V (SCE) are small.

Gibbs adsorption energy-potential and lateral interaction-potential curves

The energetics of *n*-PenOH adsorption are characterised by the magnitude of the Gibbs energy of adsorption (Fig. 12). In the limit of zero coverage the adsorption of *n*-PenOH must be described by Henry's law isotherm and the film pressure should then linearly depend on the concentration of *n*-PenOH as described by the following equation [7–10, 17–24, 55–58]:

$$\pi = RT\Gamma_{max}B_A c_A/55.5 = RT\Gamma_{max}B_A X_A \quad (9)$$

where X_A is the mole fraction of *n*-PenOH in the solution, and the adsorption equilibrium coefficient B_A (Henry isotherm) is related to the Gibbs energy of adsorption through the equation

$$\Delta G_A^\circ = -RT \ln B_A \quad (10)$$

As shown elsewhere [53–56], the values of ΔG_A° obtained according to Eqs. 9 and 10 correspond to the similar standard state as the Gibbs adsorption energy of an organic compound, obtained according to the Frumkin isotherm, being the unit mole fraction of the organic species in the bulk of the solution and a monolayer coverage of the ideal non-interacting adsorbate at the electrode surface. According to the data of Fig. 12, the

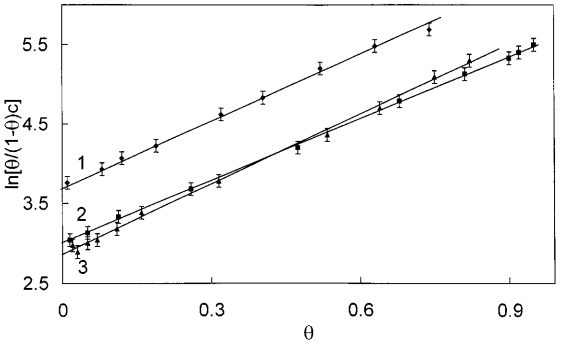

Fig. 11 Frumkin adsorption isotherm ($\omega = 0$) for *n*-PenOH adsorption on Bi single-crystal planes: (011) (*1*); (001) (*2*); (111) (*3*)

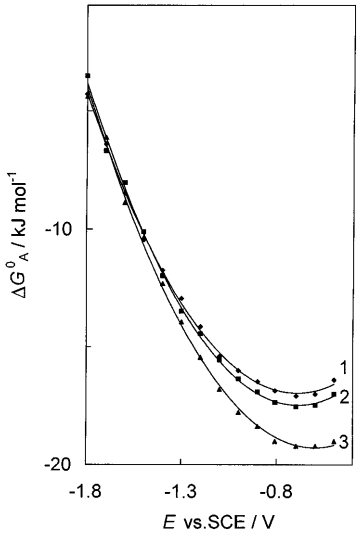

Fig. 12 Gibbs adsorption energy vs. potential curves for *n*-PenOH, obtained from chronocoulometry for Bi single-crystal planes: (111) (*1*); (001) (*2*); (011) (*3*)

ΔG_A°-E curves have a nearly parabolic shape which is in good agreement with the Frumkin-Damaskin adsorption theory [24, 27] and can be explained by the quadratic dependence of the adsorption energy of the uncharged organic compound (i.e. the adsorption equilibrium constant value) on the applied electrode potential. It must be noted that the precision of ΔG_A° values obtained by this method is improved by avoiding the differentiation of π-$\ln X_A$ plots as the values of Γ_{max}, obtained from the linear part of the π-$\ln c$ plots, are quite precise [5–8, 19–22]. Thus, the precision of the film pressure data must be very high in order to obtain the precise values of ΔG_A°. Therefore, in addition to the previously described method, the standard Gibbs energy of adsorption ΔG_A° at zero coverage as a function of the applied potential E was obtained by fitting the experimental isotherms at E = const. to the Frumkin isotherm:

$$X_A \exp\left(\frac{-\Delta G_A^\circ}{RT}\right) = \frac{\theta}{1-\theta}\exp(-2a\theta) \quad (11)$$

where a is the Frumkin interaction parameter. The values of ΔG_A° and a were obtained from the intercepts and slopes of the least-squares fittings to a straight line of $\ln[\theta/(1-\theta)c]$ versus θ plots at E = const. in the range of θ from 0.1 to 0.8. A good fit to Eq. 11 was achieved with the parameter a depending nearly parabolically on the electrode potential (Fig. 13). This result shows that the value of the projected area of the organic compound at the electrode surfaces decreases approximately linearly as the surface coverage θ increases [24, 27]. The accordance of the Gibbs energies of the *n*-PenOH adsorption, obtained from π-ln$c$ plots and from the Frumkin isotherm, is good (maximum error does not exceed ± 1.2 kJ mol^{-1}), which indicates the absence of large systematic errors in the data established. The values of ΔG_A°, obtained from π-ln$c$ plots, are always

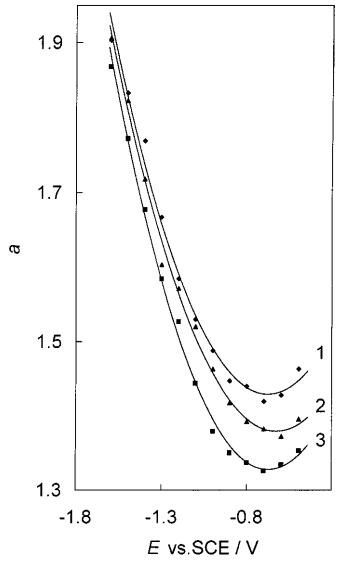

Fig. 13 Attraction interaction constant vs. potential curves for Bi(111) (*1*), Bi(001) (*2*), Bi(011) (*3*)

somewhat higher than those obtained from the Frumkin isotherm. This difference increases if the adsorption activity of the organic compound rises [6, 7], thus as its molecular weight and molar volume increases.

The adsorption data of *n*-PenOH on the Bi single-crystal planes are collated in Table 1, and show that the adsorption activity of *n*-PenOH increases in the sequence of planes $(111) < (001) < (01\bar{1})$. The surface activity of adsorbates increases in the sequence *n*-PrOH < *n*-BuOH < CH < *n*-PenOH < *n*-HexOH as the adsorption at the air | solution interface increases [1–9]. Comparison of the adsorption data of various aliphatic organic compounds shows that the value of ΔG°_{A} increases in the order of electrodes $Zn(2\bar{1}\bar{1}0) < Zn(10\bar{1}0) < Zn(0001) < Ag(110) < Ga < Ag(100) < Ag(111) < Cd(11\bar{2}0) < Cd(10\bar{1}0) < Cd(0001) < Bi(111) < Bi(001) < Hg < Bi(2\bar{1}\bar{1}) < Bi(01\bar{1}) < Sb(111) < Sb(001) < Sb(2\bar{1}\bar{1})$ as the hydrophilicity of the electrode surface decreases [2–9, 19–24, 30, 36, 37, 48].

According to Fig. 13 the lateral interaction constants *a* are positive and their values decrease when the surface charge density decreases. Also according to Fig. 13, the attractive interaction at $E_{\sigma=0}$ and at E_{max}increases in the sequence of planes $Bi(01\bar{1}) < Bi(001) < Bi(111)$. The same order of planes at E_{max} was found in the case of adsorption of *n*-PrOH, *n*-BuOH and *n*-HexOH at Bi single-crystal electrodes [1–9, 48]. In the case of adsorption of organic compounds at the metal surfaces from solution, the attractive interaction constant *a* can be expressed in terms of different particle-particle interactions at the interface [1–9, 17, 19–25, 48, 59]:

$$2a = (2Z_{W-A} - Z_{A-A} - Z_{W-W})/RT \qquad (12)$$

where Z_{i-j} is the particle-particle interaction energy, W stands for H_2O and A for adsorbate. The positive values of *a* mean that $2Z_{W-A} > Z_{A-A} + Z_{W-W}$, i.e. the adsorbate-adsorbate and water-water interactions are much more attractive than the adsorbate-water interaction. The value of *a* increases in the order of adsorbates *n*-PrOH < *n*-BuOH < *n*-HexOH ≤ *n*-PenOH < CH as the molar volume of the adsorbate molecule increases, except for *n*-HexOH. The lower value of *a* for *n*-PenOH and *n*-HexOH molecules than for CH probably indicates that the hydrocarbon tail of these compounds in the adsorption layer is not linear or that these molecules will have the more tilted orientation. If we assume at a first approximation that the water-water and the organic compound-water interactions are independent of the aliphatic compound studied, then the attraction between the adsorbed aliphatic alcohol molecules rises in the presented order of adsorbates. The same order of adsorbates is valid in the case of the adsorption of aliphatic alcohols at Hg, Zn(0001), $Zn(11\bar{2}0)$, $Zn(10\bar{1}0)$, Ag(111), Ag(110) and Ag(100) electrodes [19–24, 30, 36, 37]. The value of *a* for *n*-PenOH adsorption increases in the order of electrodes $Bi(01\bar{1}) < Bi(001) < Bi(111) < Hg < Ag(100) < Ag(111)$ [19–21, 24, 26, 43, 48].

Adsorption data for various organic compounds at the Bi single-crystal | electrolyte interface seem to conform to the prediction model [60]. The intercepts and slopes for different systems are summarised in Table 2. The slope of these plots increases, as expected, from C_3 to C_6, and the intercepts are negative and seem to decrease in the same order. The values of ρ listed in Table 2 show that, as for the Hg | solution interface [60], ρ ranges from 0 to 0.4 for the Bi single-crystal plane | aqueous electrolyte solution interface with the addition of various organic compounds. The value of ρ somewhat decreases as the length of the hydrocarbon chain or the molar volume of the compound rises, in complete agreement with theoretical predictions [60–63]. However, it is to be noted that the extrapolation procedure is very sensitive to the values of Γ_{max} or C_1, and thus only the tendency of the variation of ρ with the length or molar volume of the adsorbed molecule seems to be an object for discussion as the error in ρ is ±0.2 [60]. The values of $\rho < 1$ are in complete agreement with the results obtained from molecular models of charged interfaces [60–63]. Thus, a theoretical condition for a neutral organic adsorbate to be desorbed from the electrode surface at far negative or positive polarisations is $\Delta a = a_A - na_w < 0$ [60–63]. If Eq. 13

$$\varepsilon_i = 1 + a_i/\varepsilon_0 d S_{A,max} \qquad (13)$$

is introduced into this condition, we obtain $\Delta\varepsilon = \varepsilon_A - \varepsilon_W < 0$ and thus $\rho < 1$. The change of $\rho \leq 0.4$ for Bi | solution and Hg | solution interfaces to $\rho \geq 1.0$ at the electrolyte | air interface is difficult to explain if the same structure is assumed for these interfaces, as the maximum Gibbs excess of adsorbate Γ_{max} is approximately the same at these two interfaces [24, 43, 60]. Therefore, S_{max} is practically the same at different interfaces. Moreover, the polarizability of an organic compound a_A at $\sigma = 0$ is also independent of the interface, since it is a molecular property depending only on

Table 2 Adsorption parameters for Bi single-crystal planes obtained by the Nikitas–Pappa-Lousi model

Compound	Plane	a	b	ρ
n-PrOH	(111)	−18.2	16.6	0.32
	(001)	−14.2	14.6	0.27
n-BuOH	(111)	−20.0	25.3	0.21
	(001)	−21.8	21.3	0.26
	(01$\bar{1}$)	−18.6	22.4	0.31
n-PenOH	(111)	−21.2	26.3	0.18
	(001)	−23.1	22.8	0.23
	(01$\bar{1}$)	−18.6	20.4	0.14
n-HexOH	(111)	−22.0	27.0	0.16
	(001)	−24.0	24.0	0.21
	(01$\bar{1}$)	−20.0	22.1	0.13

the nature and molar volume of the adsorbate. Thus the dielectric constant ε_A, defined by Eq. 13, is very likely to be the same at the air | solution and Bi | solution interface ($\sigma = 0$). Similarly, ε_w is not expected to vary considerably on passing from the air | solution to the Bi | solution interface, even assuming that the H_2O molecules are in the form of monomers at the free H_2O surface and of clusters at the Bi | H_2O interface, since the formation of solvent clusters increases $S_{w,max}$ but also increases a_w, causing only small or insignificant changes in ε_w [60]. Therefore, as shown by Nikitas and Pappa-Louisi [60–63], the differences between the values of ρ at the air | solution and Bi | solution interfaces reflect the different structures of the adsorbed layer.

Conclusions

The adsorption behaviour of n-PenOH at singular Bi(111), Bi(001) and Bi(01$\bar{1}$) electrodes has been studied by CV, impedance and chronocoulometry methods. The presented results indicate that the adsorption parameters of n-PenOH depend on the crystallographic structure of the Bi planes. The adsorption parameters derived from the capacitance data at $\omega = 0$ (at $-22 < \sigma < 4\,\mu C\ cm^{-2}$) are in reasonable accordance with the data from the chronocoulometric measurements, but the difference between impedance and chronocoulometric data diminishes when the adsorption activity of the compound decreases. Accordingly, the impedance data are to some degree non-equilibrial in spite of extrapolation to $\omega \to 0$.

The comparison of the Gibbs energies of adsorption for various organic compounds shows that the adsorption activity of organic compounds at the Bi | solution interface increases in the order n-PrOH < n-BuOH < CH ≤ n-PenOH < n-HexOH as the adsorption of the organic compound at the air | solution interface rises. The difference between the adsorption activities of various Bi planes increases in the sequence of adsorbates n-PrOH < n-BuOH < CH ≤ n-PenOH < n-HexOH if the adsorption activity of the organic compound at the air | solution interface, as well as at the Bi | solution interface, rises. Thus, with the decreasing of the molar volume of adsorbate the changes in the adsorbed layer structure, caused by the adsorption of one molecule, decreases in comparison with the adsorption of larger surfactants. Comparison of the adsorption data for various aliphatic organic compounds shows that the value of ΔG_A° increases in the order of electrodes Zn(2$\bar{1}\bar{1}$0) < Zn(10$\bar{1}$0) < Zn(0001) < Ag(110) < Ga < Ag(100) < Ag(111) < Cd(11$\bar{2}$0) < Cd(10$\bar{1}$0) < Cd (0001) < Bi(111) < Bi(001) < Hg < Bi(2$\bar{1}\bar{1}$) < Bi(01$\bar{1}$) < Sb (111) < Sb(001) < Sb(2$\bar{1}\bar{1}$) as the hydrophilicity of the electrode surface decreases [19–24, 30, 36, 37].

The adsorption activity of n-PenOH at Bi(001) is very close to that for the polycrystalline bismuth solid drop electrode [11], and this result is in very good accordance with the previous conclusions [1–9, 29, 43], where it was found that the surface of the polycrystalline Bi electrode mainly consists (from 50% to 70%) of the comparatively large homogeneous surface areas (grains), adsorption characteristics of which are very close to those for the Bi(001) plane. The lower adsorption activity of Bi(111) is caused mainly, in addition to the more pronounced hydrophilicity, by a less active surface state of Bi(111), where the surface atoms are chemically saturated. The most active one is the singular Bi(01$\bar{1}$) plane, where unsaturated covalent bonds are distributed uniformly over the whole surface.

The positive values of the lateral interaction constant a for n-PenOH means that the surfactant-surfactant and water-water interactions are much more attractive than the surfactant-water interaction. At the potentials of the adsorption-desorption maxima, the molecular interaction parameter a^m decreases in the sequence of planes (001) ≥ (111) > (01$\bar{1}$) as the superficial density of the planes increases and the limiting Gibbs adsorption decreases. The dependence of the attractive interaction constant a on E is approximately parabolic and the value of a increases in the sequence of electrodes Hg < Bi(111) < Bi(001) < Bi(01$\bar{1}$) < Zn(0001) [24, 36, 37].

The value of a increases in the order of adsorbates n-PrOH < n-BuOH < n-HexOH ≤ n-PenOH < CH as the molar volume of the adsorbate molecule increases, except n-HexOH. The lower value of a for n-PenOH and n-HexOH molecules than for CH probably indicates that the hydrocarbon tail of these compounds in the adsorption layer is not linear or that these molecules will have a more tilted orientation. If we assume at a first approximation that the water-water and the organic compound-water interactions are independent of the aliphatic compound studied, then the attraction between the adsorbed aliphatic alcohol molecules rises in the presented order of adsorbates.

The limiting Gibbs adsorption Γ_{max} increases in the order of electrodes Bi(01$\bar{1}$) < Bi(111) < Bi(001) as the superficial density of planes decreases. The projected area S_{max} decreases and Γ_{max} increases in the order n-HexOH < n-PenOH < n-BuOH ≤ CH < n-PrOH. The decrease of Γ_{max} and of the limiting potential shift E_N

values, and the increase of S_{max} as the number of carbon atoms in the aliphatic alcohol molecule increases, can be explained by an increasingly tilted orientation of *n*-PenOH molecules compared with *n*-PrOH at the single-crystal Bi(001) and Bi(111) planes, as well as at Hg [7, 23, 24, 30] electrodes. Very low values of Γ_{max} and the E_N values for *n*-PrOH and *n*-HexOH at the Bi(01$\bar{1}$) plane will indicate that the *n*-PrOH and *n*-HexOH molecules probably have a practically flat orientation on the most active Bi plane investigated.

Acknowledgement This work was partially supported by the Estonian Science Foundation under Project No. 3095.

References

1. Palm UV, Pärnoja MP(1978) Sov Electrochem 14: 1070
2. Lust EJ, Palm UV(1985) Sov Electrochem 21: 1304
3. Lust EJ, Palm UV (1986) Sov Electrochem 22: 378
4. Lust EJ, Ehrlich JJ, Palm UV (1986) Sov Electrochem 22: 695
5. Lust E, Lust K, Jänes A (1995) Russ J Electrochem 31: 876
6. Lust E, Jänes A, Lust K, Miidla P(1996) J Electroanal Chem 413: 175
7. Lust E, Jänes A, Miidla P, Lust K (1997) J Electroanal Chem 425: 25
8. Lust E, Jänes A, Lust K (1997) J Electroanal Chem 437: 141
9. Lust E, Jänes A, Miidla P, Lust K (1998) J Electroanal Chem 442: 189
10. Palm UV, Damaskin BB (1977) Itogi Nauki Tekh Elektrokhim 12: 99
11. Pullerits RJ, Moldau ME, Palm UV (1975) Elektrokhimiya 11: 487
12. Ehrlich JJ, Palm UV (1974) Elektrokhimiya 10: 1866
13. Ehrlich JJ, Ehrlich TE, Palm, UV (1975) Elektrokhimiya 11: 1009
14. Palm UV, Past VE, Ehrlich JJ, Ehrlich TE (1973) Elektrokhimiya 9: 1399
15. Ehrlich JJ, Ehrlich TE, Palm UV (1978) Trans Tartu Univ 441: 87
16. Ehrlich JJ, Pärnoja MP (1975) Double layer and adsorption at solid electrodes. Tartu State University Press, Tartu p 342–345
17. Guidelli R (1980) J Electroanal Chem 110: 205
18. Guidelli R (1992) Molecular Models of Organic Adsorption at Metal-Water Interfaces. In: Lipkowski J, Ross PN (eds) Molecular adsorption at metal electrodes. VCH, New York, p 1
19. Doubova LM, Valcher S, Trasatti S (1994) J Electroanal Chem 376: 73
20. Foresti ML, Innocenti M, Guidelli R (1994) J Electroanal Chem 376: 85
21. Lipkowski J, Stolberg L (1992) Molecular Adsorption at Gold and Silver Electrodes. In: Lipkowski J, Ross PN (eds) Molecular adsorption at metal electrodes. VCH, New York, p 174
22. Trasatti S, Doubova LM (1995) J Chem Soc Faraday Trans 91: 3311
23. Damaskin B, Frumkin A, Chizov A (1970) J Electroanal Chem 28: 93
24. Damaskin BB, Petrii OA, Batrakov VV (1971) Adsorption of organic compounds on electrodes. Plenum Press, New York, pp 35–253
25. Rolle D, Schultze JW (1987) J Electroanal Chem 229: 141
26. Trasatti S (1992) Electrochim Acta 37: 2137
27. Frumkin AN (1979) Potentsialy nulevogo zaryada (potentials of zero charge). Nauka, Moscow (in Russian)
28. Frumkin A, Damaskin B, Grigoryev N, Bagotskaya I (1974) Electrochim Acta 19: 69
29. Lust E, Lust K, Jänes A, Ehrlich J (1996) Russ J Electrochem 32: 597
30. Moncelli MR, Foresti ML, Guidelli R (1990) J Electroanal Chem 295: 225
31. Grigoryev NB, Machavariani DN (1969) Elektrokhimiya 5: 87
32. Grigoryev NB, Kuprin VP, Loshkaryev YuM (1973) Elektrokhimiya 9: 1812
33. Rybalka LE, Damaskin BB, Leikis DI (1975) Elektrokhimiya 11: 9
34. Rybalka LE, Damaskin BB (1973) Elektrokhimiya 9: 1562
35. Obrastsov NB, Parfenev YuA, Danilov FI (1993) Elektrokhimiya 29: 699
36. Ipatov YuP, Batrakov VV, Shalaginov VV (1976) Elektrokhimiya 12: 286
37. Ipatov YuP, Batrakov VV (1975) Elektrokhimiya 11: 1282
38. Grigoryev NV, Kalyuzhnaya AM (1974) Elektrokhimiya 10: 1287
39. Pezzatini G, Moncelli MR, Innocenti M, Guidelli R (1990) J Electroanal Chem 295: 275
40. Vitanov T, Popov A (1976) Elektrokhimiya 12: 319
41. Khmelevaya LP, Damaskin BB (1981) Elektrokhimiya 17: 1721
42. Khmelevaya LP, Chizov AV, Damaskin BB (1978) Elektrokhimiya 14: 1304
43. Lust E, Jänes A, Lust K, Pullerits R (1997) J Electroanal Chem 431: 183
44. Weissberger A (1986) Organic solvents: physical properties and methods of purification, vol 2. Wiley, New York, p 887
45. Tedoradze GA, Arakelyan RA (1964) Dokl Akad Nauk SSSR 156: 1170
46. Armstrong RP, Race WP, Thirsk HR (1968) J Electroanal Chem 16: 517
47. Takashaki K (1968) Electrochim Acta 13: 1609
48. Lust E, Jänes A, Lust K, Väärtnõu M (1997) Electrochim Acta 42: 771
49. Hamelin A, Morin S, Richer J, Lipkowski J (1989) J Electroanal Chem 272: 241
50. Lipkowski J, Stolberg L, Yang P-F, Pettinger B, Mirwald S, Henglein F, Kolb DM (1994) Electrochim Acta 39: 1057
51. Lipkowski J, Van Houng CN, Hinnen C, Parsons R (1983) J Electroanal Chem 143: 375
52. Richter J, Lipkowski J (1988) Langmuir 2: 630
53. Richter J, Lipkowski J (1988) J Electroanal Chem 251: 217
54. Iannelli A, Richter J, Stolberg L, Lipkowski J (1990) J Plating Surf Finish 77: 47
55. Pearson WB (1972) The crystal chemistry and physics of metals and alloys. Wiley-Interscience, New York, p 280
56. Parsons R (1961) Proc R Soc London Ser A 261: 79
57. Parsons R (1964) J Electroanal Chem 7: 136
58. Parsons R (1964) J Electroanal Chem 8: 93
59. Pulidori F, Borghesani G, Pedriali R, De Battisti A, Trasatti S (1978) J Chem Soc Faraday Trans I 74: 79
60. Nikitas P, Pappa-Louisi A (1995) J Electroanal Chem 385: 257
61. Nikitas P (1988) J Electroanal Chem 263: 147
62. Nikitas P (1994) J Phys Chem 98: 6577
63. Nikitas P (1994) Electrochim Acta 39: 865